Controllable Expansion of Single-Walled Carbon Nanotube Dispersions Using Density Gradient Ultracentrifugation

Pei Zhao[†], Erik Einarsson[†], Rong Xiang[†], Yoichi Murakami[‡], Shigeo Maruyama[†]*

[†]Department of Mechanical Engineering, The University of Tokyo,

7-3-1 Hongo, Bunkyo-ku, Tokyo 113-8656, Japan

[‡]Global Edge Institute, Tokyo Institute of Technology,

2-12-1 Ookayama, Meguro-ku, Tokyo 152-8550, Japan

*Author email: maruyama@photon.t.u-tokyo.ac.jp

TEL: +81-3-5841-6421   FAX: +81-3-5800-6983

ABSTRACT. We present a protocol to selectively isolate single-walled carbon nanotubes (SWNTs) with different chiralities in a full-colored "rainbow" expansion using density gradient ultracentrifugation (DGU). Starting with SWNTs synthesized by the alcohol catalytic chemical vapor deposition (ACCVD) method, we used *sodium deoxycholate* (DOC) and *sodium dodecyl sulfate* (SDS) as co-surfactant encapsulating agents to form a DOC-restricted SDS wrapping morphology around the SWNTs. This enhances the density differences between nanotubes of different diameters, which leads to efficient chirality redistribution when combined with an appropriate density gradient profile. UV-Vis-NIR absorbance spectra and photoluminescence excitation (PLE) maps show the optical properties of each fraction, and 97% pure isolation of (6,5) SWNTs achieved from the rainbow is also reported.

Introduction

The single-walled carbon nanotube (SWNT), which is usually thought of as a sheet of graphene rolled into nanometer-sized cylinder, has been the subject of intense research since it was first discovered in 1993.[1] SWNTs have attracted enormous scientific attention on account of their extraordinary electrical, optical and mechanical properties resulting from their quasi-one-dimensional structure.[2] However, the development of SWNTs into novel devices still faces several challenges, not least of which is the controlled growth of SWNTs with specific structures or properties. Selective synthesis of SWNTs with a certain chirality or electronic character has yet to be realized, and it is still unclear whether or not such a method could scale to produce the large amount of type-selected SWNTs necessary for some of their most promising potential applications. Realizing this goal, either by controlled growth or post-growth processing, makes SWNT research remain one of the hottest topics in nanotechnology and science today.

Several groups have made some breakthroughs showing that preferential growth of SWNTs with a narrow chirality distribution is possible using a common chemical vapor deposition (CVD) technique.[3-5] However, the reproducibility of such synthesis methods highly depends on the CVD conditions, which differ from laboratory to laboratory. Moreover, problems associated with single-chirality controlled synthesis of SWNTs still constitute one of the main obstacles to using this material in further applications. In this sense, even though further development of large-scale application of SWNTs with specific structures will be mostly by direct synthesis, post-growth treatment by physical or chemical techniques is expected to have an important role to play.

There are a number of methods for separating SWNTs, such as dielectrophoresis,[6] electrophoresis,[7] covalent surface functionalization,[8] and non-covalent chemical treatments.[9-14] These sorting techniques have led to a tremendous rise in theoretical and experimental research investigating SWNTs for applications such as field emission transistors,[15] transparent thin films,[16] identification of

photoluminescence sidebands,[17] etc. Among these sorting methods, density gradient ultracentrifugation[10,18] (DGU), a surfactant-based technique, has proven to be effective in yielding high-quality SWNTs without intensive or complicated chemical or physical treatments. Due to the combination of low cost, scalability, easy operability, and high yield, the DGU approach has become the most commonly used technique among researchers to separate as-grown SWNTs to satisfy their needs in exploring the novel properties of this new material.[19-21]

Since SWNTs themselves are hydrophobic, this DGU separation is achieved by structure-dependent wrapping of ionic surfactants to realize the hydrophilicity, which at the same time changes the buoyant densities of mixed SWNTs and facilitates their separation in a density-gradient medium. Although the overall separation process is conceptually rather simple, suitable recipes for dispersing surfactants and density gradient profiles to enable a proposed sorting of SWNTs have been dedicatedly investigated for years. Another critical issue is related to the further understanding of surfactant environments and their interaction with SWNTs. This understanding will hinge on our ability to chemically tune the efficient sorting of SWNTs for more chiralities and structures.[21] For example, M. Hersam et al. have shown that the participation of both *sodium cholate* (SC) and *sodium dodecyl sulfate* (SDS) is critical for a successful DGU separation, and combined with a density gradient profile the ratio of these two surfactants also determines the sorting result (i.e., by diameter or by electronic type).[10] Meanwhile, results from the Los Alamos group headed by S. Doorn indicate that the involvement of an electrolyte, such as NaCl, can lead to enhanced adsorption of SDS, resulting in separation by electronic type in the absence of SC.[20] The differences in these reports, which realized essentially the same separation in different surfactant and dielectric environments, suggest that the mechanisms involved in the DGU technique are not yet fully understood.

Here we present a protocol to controllably obtain a polychromatic "rainbow" dispersion containing seven different colored layers. This was achieved by the DGU method using a co-surfactant system containing *sodium deoxycholate* (DOC) and *sodium dodecyl sulfate* (SDS). We report our findings based on spectroscopic analysis of the seven separated layers and investigate the surfactants' roles in

realizing this separation. We also propose a model to explain this separation mechanism: DOC-restricted SDS wrapping of SWNTs.

Experimental

A density gradient column was formed in a polycarbonate centrifuge tube by layering, from top to bottom, equal amounts of 20, 30, and 40% w/v iodixanol. Each layer contained 1.5% w/v SDS. SWNTs synthesized by the alcohol catalytic chemical vapor deposition (ACCVD) method[3,22] were dispersed in a mixture of D_2O and 0.5% w/v DOC, followed by horn sonication and centrifugation. The supernatant was then carefully mixed with SDS-containing iodixanol and inserted 2/3 of the way down the density gradient column. DGU was performed at 197,000 g for 22 h using a Hitachi-Koki S52ST swing-bucket rotor. After centrifugation, each of the resulting layers was extracted and collected using a micropipette, and then diluted by surfactant-contained D_2O to an amount suitable for spectroscopic measurement (under normal conditions every 150 μL needed to be diluted to 1 mL).
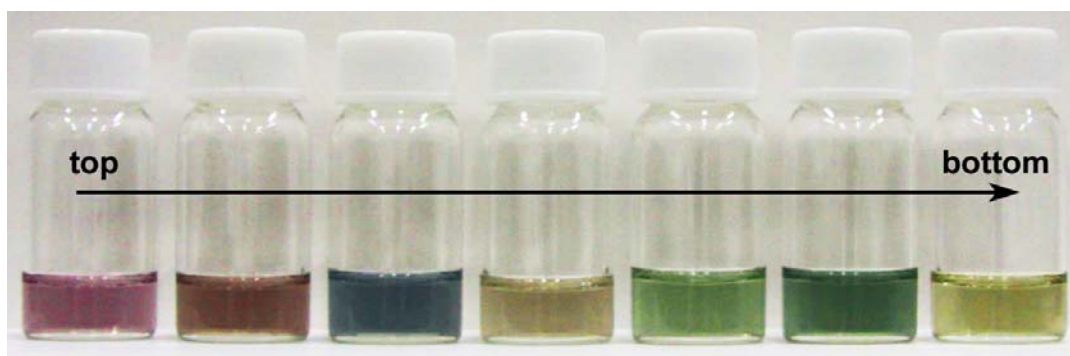
Using D_2O with 0.1% w/v DOC and 1.33% w/v SDS as the baseline, we measured the optical absorbance using an ultraviolet-visible-near infrared spectrometer (UV-vis-NIR, UV-3150, Shimazdu) after fractionating four distinguished layers from DGU columns. Photoluminescence excitation (PLE) spectra were also recorded by a HORIBA Fluorolog Spectrometer equipped with a liquid nitrogen cooled detector.
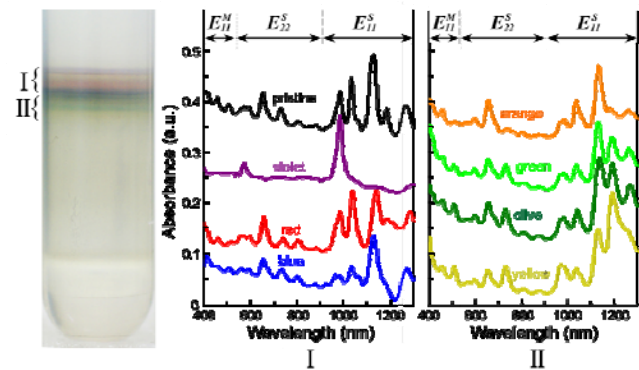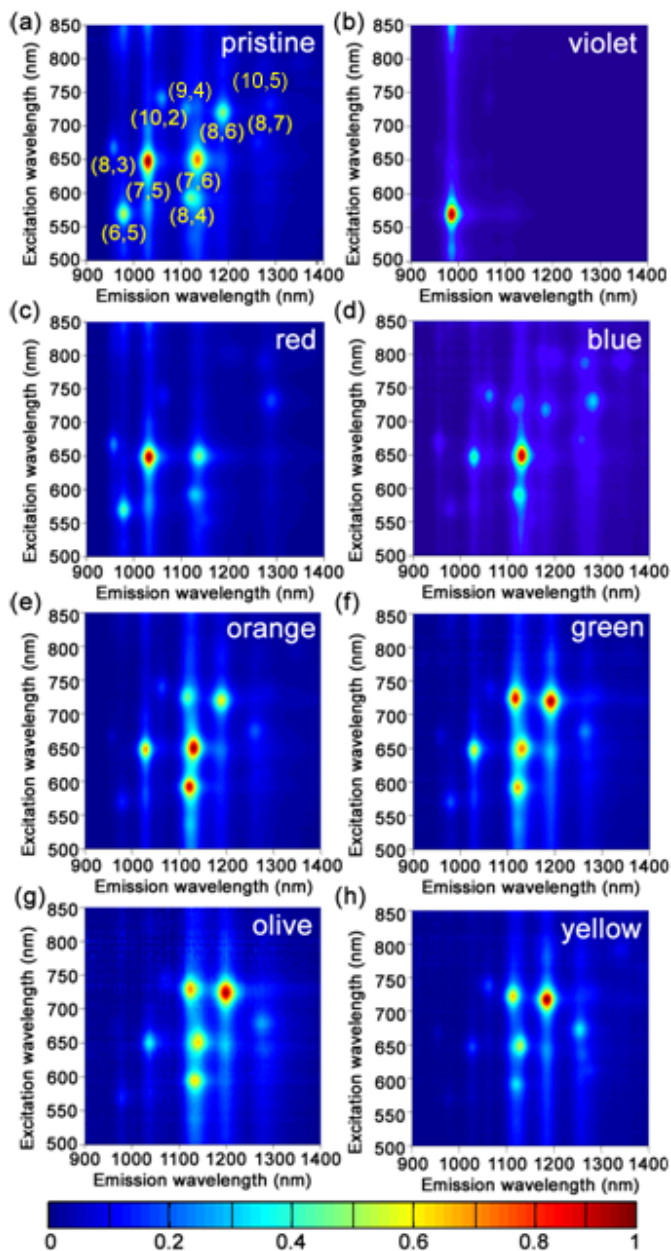

Figure 1. Left: Photograph showing multilayered separation "rainbow" of ACCVD SWNTs by density gradient ultracentrifugation. Right: Optical absorbance spectra of each colored fraction. Graph I shows the spectra from the pristine sample plus the topmost three colored layers. The spectra corresponding to the lower four layers are shown in graph II.

Results and Discussion

Figure 1 shows a photograph (left) of the rainbow of layers resulting from this dual-surfactant DGU separation process. UV-Vis-NIR absorbance spectra (right) were obtained from each of the seven layers, which were fractioned and diluted with D_2O to obtain sufficient volume to measure. Each spectrum is presented using approximately the same color as it appears to the eye, and the spectrum from the initial dispersion (i.e., prior to DGU) is shown for reference. These absorbance spectra show that the chiralities in the pristine sample are efficiently redistributed during DGU, and this redistribution has a strong dependence on the structure of the isolated species. The topmost violet layer contains primarily (6,5) SWNTs, which have the smallest diameter of those detected in the sample. The dominant species in each successive layer has an increasingly larger diameter, showing the redistribution is diameter-selective and separation is driven by difference in buoyant density. To illustrate the multiple colors, layers from several samples were collected from several runs, demonstrating the good reproducibility. The collected volumes are shown in Figure 2. Similar results were obtained using HiPCO and CoMoCAT SWNTs, with some of the layers changing or missing depending on the different diameter distributions in the starting material (see Supporting Information).

Figure 2. SWNT dispersions sorted by the density gradient ultracentrifugation (DGU) method. "Top" and "bottom" indicate the relative position of each color in the DGU column, and each color is dominated by SWNTs of a different diameter.
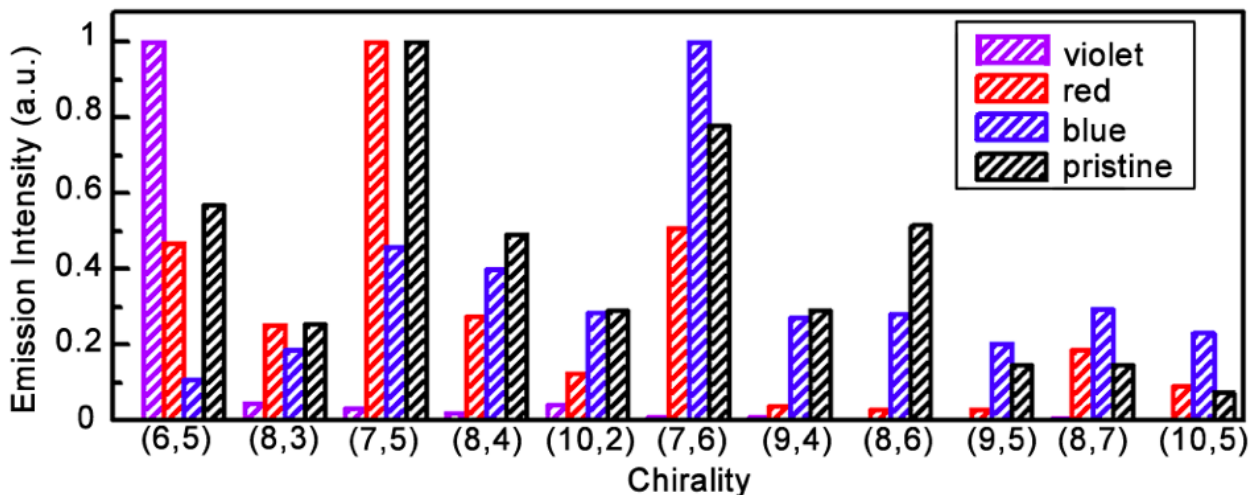
Figure 3. Normalized photoluminescence excitation (PLE) maps of the initial dispersion (a) and all the post-DGU layers (b-h).

As with the absorbance spectra, photoluminescence excitation (PLE) maps[23] were obtained from each of the fractioned layers, and also illustrate the unique composition of each layer. In Figure 3, the PLE map obtained from the pristine sample (a) is compared to those of all seven sorted layers (b-h). These maps illustrate the excellent isolation of (6,5) and good enrichment of (7,5) and (7,6) from the initial dispersion. The most notable aspect of this result is that (6,5) is one of the minority species in the ACCVD starting material, yet is selected with very high purity. Unlike previous studies[10,18] using CoMoCAT SWNTs—of which (6,5) SWNTs are known to be the dominant chiral species—this effective extraction of a minority fraction of the sample clearly shows the efficient diameter selection by this dispersion process.

Normalized emission intensities of the initial dispersion and the first three layers are plotted in Figure 4. The best selectivity was found for (6,5) SWNTs, which dominated the topmost violet layer. (7,5) and (7,6) SWNTs were preferentially sorted into the subsequent red and blue layers, respectively. It is important to note that a gap exists between the violet layer and the rest of the layers, which is due to a sizeable density difference (approximately 0.006 g/mL). The emission intensity of this gap layer is also much weaker than its highly concentrated neighbors (see Supporting Information),

Figure 4. Normalized photoluminescence emission intensities of violet, red and blue layers, which are enriched with (6,5), (7,5) and (7,6) SWNTs, respectively. Emission intensities from the starting material are also shown for reference.

indicating a very low population of SWNTs in this region. This gap effectively creates a buffer layer that isolates the violet (6,5) fraction from the rest of the dispersion, making (6,5) SWNTs the simplest to extract in high purity without needing to perform multiple iterations.[10]

The degree of (6,5) isolation achieved in the violet fraction is as high as 97%. This was determined from the PLE peak intensities, which were normalized by the theoretical PL intensities as calculated by Oyama et al.[24] We acknowledge this renormalization may not be entirely accurate, as the model[24] is still preliminary, however the trend in both chirality and diameter dependence is in good agreement with direct experimental measurements of SWNT intrinsic fluorescence action cross sections (see Supporting Information).[25] Because of its high purity, this sample has been used to provide direct evidence[17] for phonon sidebands in PL emission.[26] Furthermore, the retention of the total amount present in the initial dispersion is approximately 50%, quantifying the efficient selection by this method. However, with the increase of diameter in subsequent layers the isolation of specific chiralities gets progressively worse, due to the diversification of chiralities (and more possible chiral angles) corresponding to similar diameters. From the absorbance spectra in Figure 1 we can see that metallic nanotubes exist in all the layers except for the topmost violet layer. Without further measurements the fate of metallic nanotubes

cannot be addressed in detail, but since the separation is diameter dependent it is reasonable to assume that the distribution of metallic SWNTs in the density gradient may be similar to that of semiconducting SWNTs.

This rainbow dispersion can also be useful in studying the interaction between nanotubes and surfactants. By changing the surfactant environment and observing the expansion/contraction of the layers, or shifting of their positions, the influence of the surfactants on the SWNT buoyancy can be determined (see Supporting Information). Based on our observations we propose the following mechanism. The strong interaction between the

Figure 5. Schematic depiction of the morphology of surfactant wrapping around a (6,5) nanotube (a) by SDS only; (b) by DOC only; (c) by DOC followed by SDS. The hydration layers of the micelles are not shown (see text). The thin, red shape indicates SDS, while the thicker, blue shape denotes DOC. Filled circles denote the surfactant heads.

hydrophobic part of DOC and the nanotube sidewall[21] causes DOC to wrap around the nanotube with a preferred orientation. TEM observation of SWNTs obtained from the violet layer appears to show surfactant wrapping, in agreement with numerical simulations[21] (see Supporting Information). It is known that SDS-wrapped SWNTs have higher density than DOC-wrapped SWNTs because of their smaller micelle sizes formed by hydrated molecules.[21,27,28] Hence, we expect a co-surfactant wrapping to have intermediate density. However, we hypothesize that SDS, which is introduced after DOC, fills the space between DOC molecules. We note that the pattern of SDS in Figure 5(c) is just to illustrate the morphology should be different from that in Figure 5(a), and does not necessarily represent the true orientation of the molecules. Most importantly, the space between DOC molecules that is accessible to SDS depends on the SWNT diameter, leading to a diameter-dependent enhancement in the density difference among SWNTs. This causes the expansion of the entire rainbow region after DGU. The
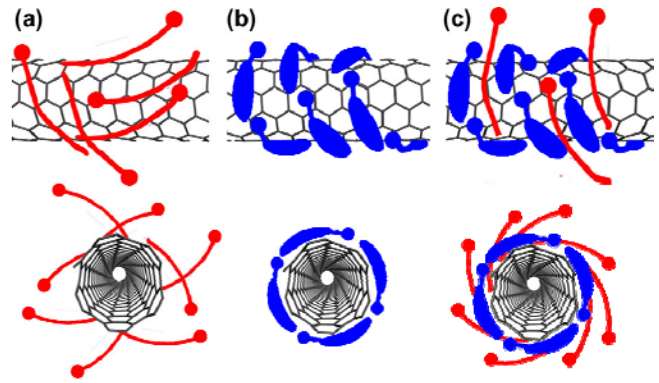
density difference can be further exaggerated and the layers expanded by choosing an appropriate density gradient profile.

Conclusions

In summary, we report enhanced diameter-dependent selectivity of SWNTs using a dual-surfactant DGU process, which produced a full rainbow of colored layers from a dispersion of ACCVD SWNTs. This method shows excellent selection and retention of (6,5) nanotubes, despite being a minority fraction of the starting material. A model for the separation mechanism is also proposed, which explains the roles of the two different surfactants. This method not only illustrates the potential for complete isolation of a single (n,m) species, but also provides a simple way to better understand surfactant-nanotube interactions. We believe that further understanding and refinement of this process can lead to higher purity extraction of single-chirality SWNTs.

Supporting Information Available: Experimental details, TEM images of the (6,5) nanotube, separation of HiPCO and CoMoCAT nanotubes, modification of rainbow layers, and pre- and post-centrifugation density gradient profiles. This material is available free of charge via the Internet at http://pubs.acs.org.

References:

  (1) Iijima, S.; Ichihashi, T. *Nature* **1993**, *363*, 603.

(2) Jorio, A.; Dresselhaus, G.; Dresselhaus, M. S. *Carbon Nanotubes: Advanced Topics in the Synthesis, Structure, Properties and Applications (Topics in Applied Physics)* (Springer, **2008**).

(3) Miyauchi, Y.; Chiashi, S.; Murakami, Y.; Hayashida, Y.; Maruyama, S. *Chem. Phys. Lett.* **2004**, *387*, 198.

(4) Li, X.; Tu, X.; Zaric, S.; Welsher, K.; Seo, W. S.; Zhao, W.; Dai, H. *J. Am. Chem. Soc.* **2007**, *129*, 15770.

(5) Chiang, W. H.; Sankaran, R. M. *Nat. Mater.* **2009**, *8*, 882.

(6) Krupke, R.; Hennrich, F.; Löhneysen, H. V.; Kappes, M. M. *Science* **2003**, *301*, 344.

(7) Usrey, M. L.; Lippmann, E. S.; Strano, M. S. *J. Am. Chem. Soc.* **2005**, *127*, 16129.

(8) Banerjee, S.; Hemraj-Benny, T.; Wong, S. S. *Adv. Mater.* **2005**, *17*, 17.

(9) Chen, Z.; Du, X.; Du, M.; Rancken, C. D.; Cheng, H.; Rinzler, A. G. *Nano Lett.* **2003**, *3*, 1245.

(10) Arnold, M. S.; Green, A. A.; Hulvat, J. F.; Stupp, S. I.; Hersam, M. C. *Nat. Nanotechnol.* **2006**, *1*, 60.

(11) Zheng, M.; Jagota, A.; Strano, M. S.; Santos, A. P.; Barone, P.; Chou, S. G.; Diner, B. A.; Dresselhaus, M. S.; Mclean, R. S.; Onoa, G. B.; Samsonidze, Ge. G.; Semke, E. D.; Usrey, M.; Walls, D. J. *Science* **2003**, *302*, 1545.

(12) Tu, X.; Zheng, M. *Nature* **2009**, *460*, 250.

(13) Ju, S.-Y.; Doll, J.; Sharma, I. Papadimitrakopoulos, F. *Nat. Nanotechnol.* **2008**, *3*, 356.

(14) Nish, A.; Hwang, J.-Y.; Doig, J.; Nicolas, R. J. *Nat. Nanotechnol.* **2007**, *2*, 640.

(15) Engel, M.; Small, J. P.; Steiner, M.; Freitag, M.; Green, A. A.; Hersam, M. C.; Avouris, Ph. *ACS Nano* **2008**, *2*, 2445.

(16) Green, A. A.; Hersam, M. C. *Nano Lett.* **2008**, *8*, 1417.

(17) Murakami, Y.; Lu, B.; Kazaoui, S.; Minami, N.; Okubo, T.; Maruyama, S. *Phys. Rev. B* **2009**, *79*, 195407.

(18) Arnold, M. S.; Stupp, S. I.; Hersam, M. C. *Nano Lett.* **2005**, *5*, 713.

(19) Yanagi, K.; Miyata, Y.; Kataura, H. *Appl. Phys. Express* **2008**, *1*, 034003/1.

(20) Niyogi, S.; Densmore, C. G.; Doorn, S. K. *J. Am. Chem. Soc.* **2009**, *131*, 1144.

(21) Arnold, M. S.; Suntivich, J.; Stupp, S. I.; Hersam, M. C. *ACS Nano* **2008**, *2*, 2291.

(22) Maruyama, S.; Kojima, R.; Miyauchi, Y.; Chiashi, S.; Kohno, M. *Chem. Phys. Lett*. **2002**, *360*, 229-234.

(23) Bachilo, S. M.; Strano, M. S.; Kittrell, C.; Hauge, R. H.; Smalley, R. E.; Weisman, R. B. *Science* **2002**, *298*, 2361-2366.

(24) Oyama, Y.; Saito, R.; Sato, K.; Jiang, J.; Samsonidze, Ge. G.; Grüneis, A.; Miyauchi, Y.; Maruyama, S.; Jorio, A.; Dresselhaus, G.; Dresselhaus, M. S. *Carbon* **2006**, *44*, 873-879.

(25) Tsyboulski, D. A.; Rocha, J-D. R.; Bachilo, S. M.; Cognet, L.; Weisman, R. B. *Nano Lett.* **2007**, *7*, 3080-3085.

(26) Torrens, O. N.; Zheng, M; Kikkawa, J. M. *Phys. Rev. Lett.* **2008**, *101*, 157401-1-157401-4.

(27) Fontell, K. Kolloid-Z. u. Z. Polymere **1971**, *246*, 614-625.

(28) Mukerjee, P. J. Colloid. Sci. **1964**, *19*, 722-728.

FIGURE CAPTIONS

Figure 1. Left: Photograph showing multilayered separation "rainbow" of ACCVD SWNTs by density gradient ultracentrifugation. Right: Optical absorbance spectra of each colored fraction. Graph I shows the spectra from the pristine sample plus the topmost three colored layers. The spectra corresponding to the lower four layers are shown in graph II.

Figure 2. SWNT dispersions sorted by the density gradient ultracentrifugation (DGU) method. "Top" and "bottom" indicate the relative position of each color in the DGU column, and each color is dominated by SWNTs of a different diameter.

Figure 3. Normalized photoluminescence excitation (PLE) maps of the initial dispersion (a) and all the post-DGU layers (b-h).

Figure 4. Normalized photoluminescence emission intensities of violet, red and blue layers, which are enriched with (6,5), (7,5) and (7,6) SWNTs, respectively. Emission intensities from the starting material are also shown for reference.

Figure 5. Schematic depiction of the morphology of surfactant wrapping around a (6,5) nanotube (a) by SDS only; (b) by DOC only; (c) by DOC followed by SDS. The hydration layers of the micelles are not shown (see text). The thin, red shape indicates SDS, while the thicker, blue shape denotes DOC. Filled circles denote the surfactant heads.

TOC image
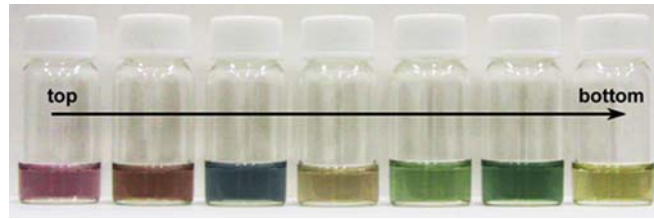
SUPPORTING INFORMATION

Controllable Expansion of Single-Walled Carbon Nanotube Dispersions

Using Density Gradient Ultracentrifugation

Pei Zhao, Erik Einarsson, Rong Xiang, Yoichi Murakami, Shigeo Maruyama

I. EXPERIMENTAL DETAILS

Sample layer:

7.5 mg ACCVD-SWNTs were dispersed in 6 mL D_2O containing 0.5% w/v (0.03g) *sodium deoxycholate* (DOC). The dispersion was then bath sonicated for 10 min, followed by horn ultrasonication for 1 hour (UP-400s, Hielscher Ultrasonics, 1 cycle, 400 W). The suspension was put into 4.5 mL glass centrifuge tubes (1.4 mL each, total amount is 5.6 mL, some of the suspension may vaporize during ultrasonication), then ultracentrifuged at 78 krpm (276,000 g) at 22 ^{o}C (Hitachi CS 100GXL) for 15 min, using an angle rotor (Hitachi-Koki S100AT), both acceleration and deceleration values were set to 9 (maximum). The upper portion of the supernatant was taken (0.875 mL from each tube, total amount is 3.5mL), and mixed with 3.5 mL of 60% iodixanol and 0.07 g *sodium dodecyl sulfate* (SDS), and then horn ultrasonicated for another 30 min. At this time the DOC concentration in the sample layer is 0.25% w/v.

Density gradient:

Density gradient layers of 20, 30, and 40% concentration were prepared with 1.5% w/v SDS each and bath sonicated them for 1 hour. Using plastic test tubes (5mL), a 40% layer was put at the bottom, followed by a 30% layer and then a 20% layer on top of that. The upper layers were both deposited drop by drop so as to minimize mixing. The tubes were then sealed, and laid horizontally for 1 hour to make a continuous density gradient.

Ultracentrifugation process:

Using a syringe needle, 1.5 mL of the SWNT dispersion was added into each density gradient tube (within the 30% iodixanol layer). The capsules were then placed in a swing rotor (Hitachi-Koki S52ST), and ultracentrifuged at 52 krpm (197,000g) at 15 ^{o}C for 22 hours. In this case the acceleration and deceleration value was set to five.

Controllable overall expansion:

During the preparation of the inserted sample layer, which contains equal volumes of unbundled SWNT dispersion and 60% iodixanol, the amount of SDS that contained in this layer was either 0% (no SDS), 1%, 1.25%, or 1.5% w/v. Insertion of this layer was followed by 1 hour of horn-type ultrasonication. All other DGU parameters were kept the same as in the previous section. Results are shown in Figure S5. Our hypothesis is that DOC packs in higher density on small diameter SWNTs, leaving less open space for subsequent SDS binding than is available on large diameter SWNTs. In this case, increased SDS concentration leads to more SDS binding to large diameter nanotubes, which increases their densities and drives them further down the density gradient (as seen in Fig. S5). Small diameter SWNTs, however, are relatively unaffected by the SDS concentration.

HiPCO/CoMoCAT SWNTs DGU preparation:

3.0 mg HiPCO/CoMoCAT-SWNTs were dispersed in 6 mL D_2O containing 0.5% w/v DOC. The dispersion was then bath sonicated for 10 min, followed by horn ultrasonication for 1 hour. The suspension was then ultracentrifuged at 78 krpm (276,000 g) at 22 ^{o}C (Hitachi CS 100GXL) for 30 min using an angle rotor. The following procedures are identical to the ACCVD-SWNTs DGU preparation. Results shown in Figure S6.

Fraction collection:

A micro-pipette was used to fractionate the final dispersion, which was taken out in 20 µL sections. Each fraction was diluted to a concentration appropriate for subsequent spectroscopic analysis.

Spectroscopy:

D$_2$O containing 0.1% w/v DOC and 1.33% w/v SDS was used as the baseline of UV-Vis-NIR absorbance (UV-3150, Shimadzu). Samples were also characterized by photoluminescence excitation (PLE, Fluorolog, HORIBA) and TEM (JEOL 2000EX, operated at 120 kV).
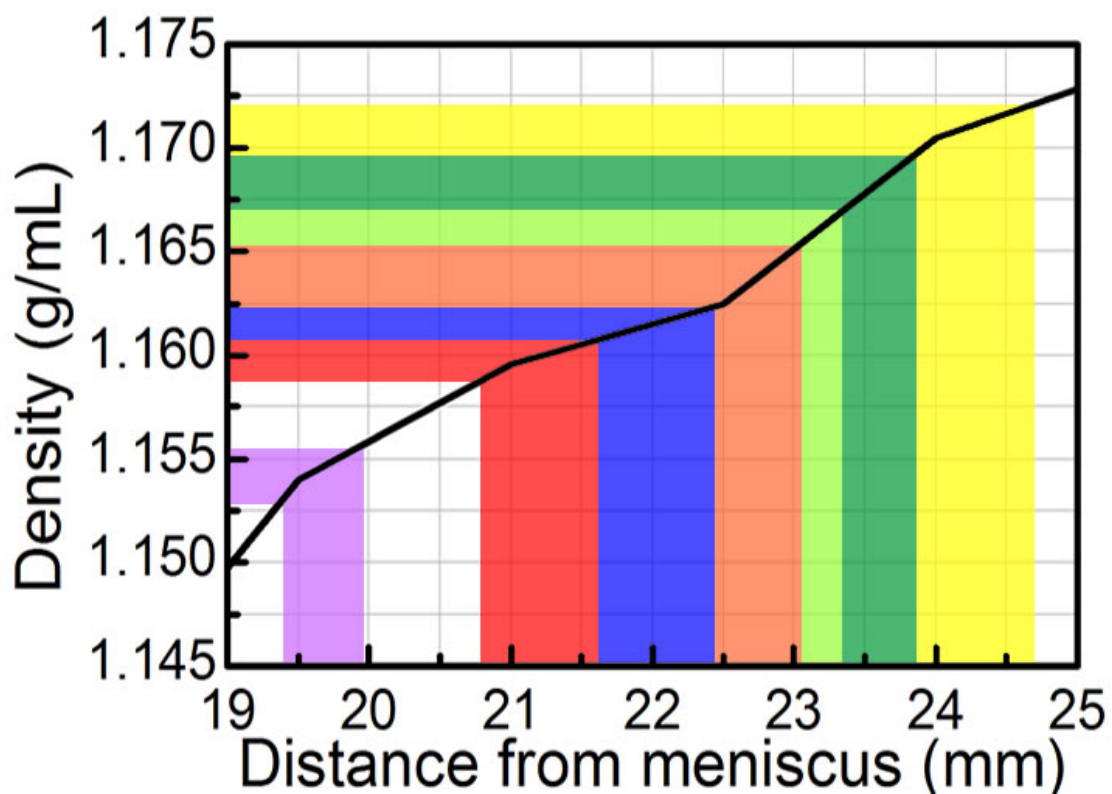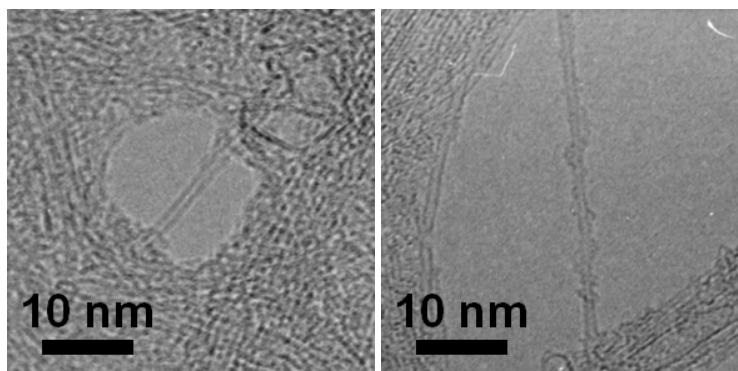
II. SUPPORTING FIGURES
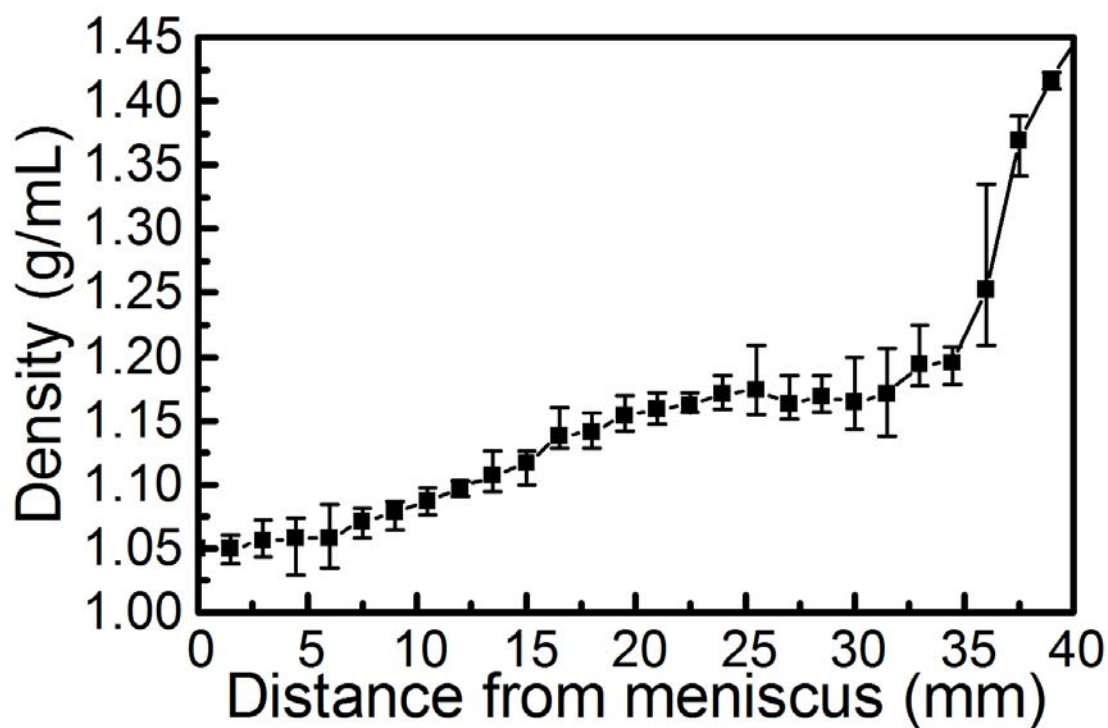
**Figure S1.** Density gradient distribution after ultracentrifugation. The volume of each layer is 150 μL.

Figure S2. Density gradient fractions with different colors, with mm scale bar (zero is at bottom of the meniscus).


Figure S3. Colored fractions and their corresponding densities in the DGU tube.

Figure S4. Transmission electronic microscopy images of SWNTs extracted from the violet fraction. The sample was rinsed thoroughly prior to observation to remove as much iodixanol as possible.
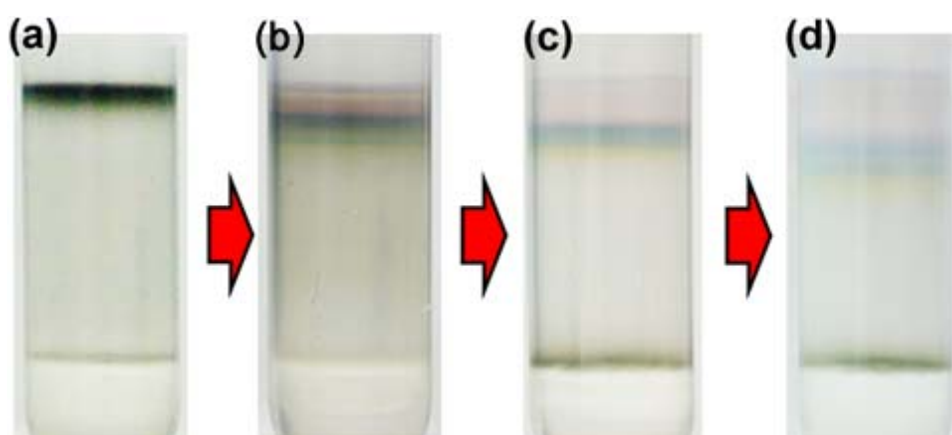

Figure S5. Controllable overall expansion of layers by adjusting surfactant concentration. Concentrations of SDS are (a) 0.0%, (b) 1.0%, (c) 1.25%, and (d) 1.5% respectively.
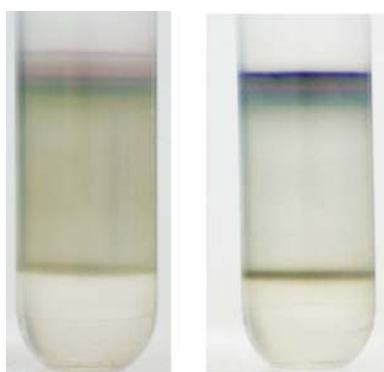
Figure S6. Expansion of HiPCO (left) and CoMoCAT (right) SWNTs. A highly concentrated violet (6,5) layer is apparent in the CoMoCAT expansion.
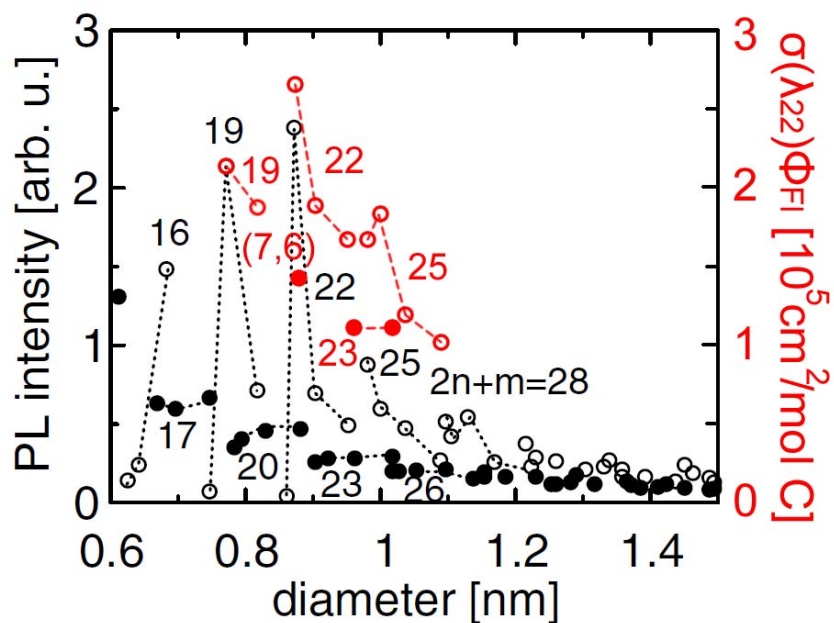
Figure S7. Comparison of SWNT calculated PL intensities from Ref. [24] (black) and PL action cross sections from Ref. [25] (red). Type I and type II are denoted by open and solid dots, respectively.
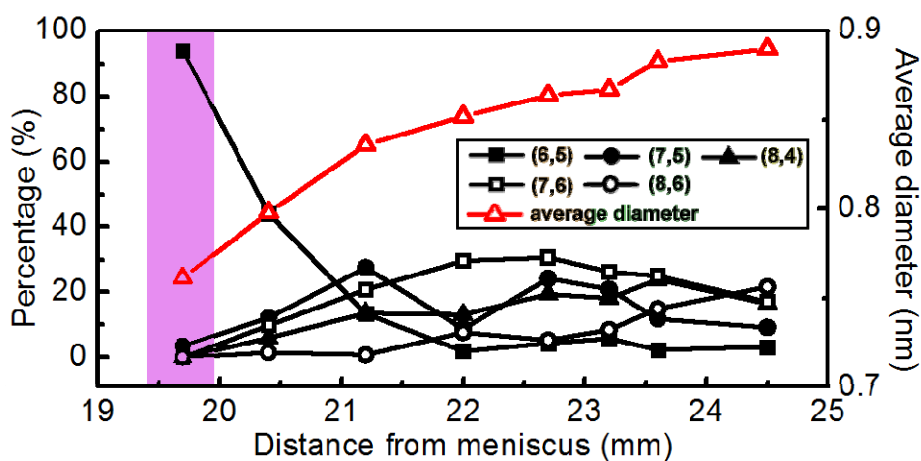
Figure S8. Abundance of dominantly selected (*n,m*) semiconducting nanotube species and their average diameters in the resulting colored fractions. Percentages were calculated from experimental PLE intensities normalized by theoretical PLE intensities [24].